PHYSICAL REVIEW B VOLUME 41, NUMBER 12 15 APRIL 1990-II

Scattering-matrix formulation of curved-wave multiple-scattering theory: Application to x-ray-absorption fine structure

J. J. Rehr
Department of Physics, FM-15, University of Washington, Seattle, Washington 98195

R. C. Albers
Theoretical Division, Los Alamos National Laboratory, Los Alamos, New Mexico 87545

(Received 13 January 1989; revised manuscript received 4 January 1990)

Curved-wave multiple-scattering contributions to XAFS (x-ray-absorption fine structure) are calculated with use of an efficient formalism similar to that based on the plane-wave approximation, but with scattering amplitudes $f(\theta)$ replaced by distance-dependent "scattering matrices" $F_{\lambda,\lambda'}(\rho,\rho')$. Here $\rho = k\mathbf{R}$, k being the photoelectron wave number and $\mathbf{R}$ is a bond vector, while the matrix indices $\lambda=(\mu,\nu)$ represent terms in a convergent expansion that generalizes the small-atom approximation. This approach is based on an exact, separable representation of the free propagator (or translation operator) matrix elements, $G_{L,L'}(k\mathbf{R})$, in an angular momentum $L=(l,m)$ and site basis. The method yields accurate curved-wave contributions for arbitrarily high-order multiple-scattering paths at all positive energies, including the near-edge region. Results are nearly converged when the intermediate λ summations are truncated at just six terms, i.e., (6×6) matrices. The lowest-order (1×1) matrix $F_{00,00}$ is the effective, curved-wave scattering amplitude, $f(\rho,\rho',\theta)$, and yields a multiple-scattering expansion equivalent to the point-scattering approximation. Formulas for multiple-scattering contributions to XAFS and photoelectron diffraction are presented, and the method is illustrated with results for selected multiple-scattering paths in fcc Cu.

I. INTRODUCTION

The standard theory of x-ray-absorption fine structure (XAFS) used for structural analysis is based upon a multiple-scattering formalism.[1,2] In addition to the first-order or single-scattering term needed to determine nearest-neighbor distances, higher-order multiple-scattering contributions are often important in quantitative calculations of XAFS. They can be significant just above the absorption edge in the XANES (x-ray-absorption near-edge structure) region, as well as at high energies, extending into the EXAFS (extended XAFS) region. Multiple-scattering terms are also required for extracting more subtle structural information such as second- and third-nearest-neighbor distances and bond angles.

Implicit in the standard theory of XAFS is the assumption of a spherical muffin-tin scattering potential; i.e., the potential seen by the photoelectron is composed of nonoverlapping, spherically symmetric potentials around each atom and is flat between the different atomiclike potentials. The energies are usually chosen so that this flat region defines zero energy, i.e., the muffin-tin zero. Although one can question the adequacy of this type of potential for certain systems (e.g., small molecules), especially at low or near-edge photoelectron energies, we will ignore this point here. Instead, we shall simply assume the canonical muffin-tin potential and concentrate on the solution of the multiple-scattering problem.

There have been many approaches to the multiple-scattering problem.[1-5] In solving for the ground-state electronic structure of solids and molecules, e.g., one typically reduces the problem to an exact diagonalization based upon some assumed wave-function basis set. A similar approach has been used for XAFS calculations with excellent results using both cluster[3] and band-structure[4] methods, particularly in the near-edge region where multiple-scattering effects are expected to be strongest. At energies high above the absorption edge (the EXAFS region), the excited electron has high kinetic energy that in turn requires either many plane waves or many orbital angular-momentum components (or both) for an adequate representation. This dramatically increases the size of the matrices that need to be diagonalized (for which the computational time scales as the cube of the matrix size) until such calculations exceed the capabilities of present computers. This sets an upper limit to the energies for which such an approach is feasible.

An alternative approach to the multiple-scattering problem is based on perturbation theory[1-2,5] in the strength of the scattering potential. We refer to this method as a "path" approach, since the perturbation expansion can be expressed in terms of a hypothetical path that an electron follows as it scatters and propagates from atom to atom. Indeed, this is the basis for the standard XAFS formalism used for structural analysis, in which the perturbation theory is truncated at the first scattering term. The path approach works well in the high-energy region, where multiple-scattering corrections are weaker and where a simplifying plane-wave approximation becomes increasingly accurate. Its chief drawback has been that only relatively low-order (at most triple-scattering[5]) terms have been possible to calculate exactly in an efficient tractable form. The main goal in the present paper is to remedy this limitation and thus permit calculations to arbitrary order.

One might expect that a path formalism would always be inferior relative to the diagonalization approaches in (low-energy) regimes where the usual basis sets converge well. In that case diagonalization is virtually exact and hence is equivalent to summing the path formalism to infinite order,[2] while a direct calculation using the path formalism must necessarily truncate at some finite order. This contrast shows up most transparently in the Korringa-Kohn-Rostoker (KKR) band-structure method for calculating the electronic structure of periodic solids, where one can explicitly and analytically sum the paths to infinite order to produce the KKR equations. What makes the path formalism competitive for a number of important positive energy applications such as XAFS and photoemission are the various lifetime effects that smear out the exact results. In these applications only unoccupied electronic structure is probed, i.e., electronic states with energies above the Fermi energy. Final-state lifetime effects then allow one to truncate the multiple-scattering expansion such that only path lengths less than a few mean free paths are retained. In practice, the importance of long paths can be gauged by the Fourier transform, $\tilde{\chi}(R)=\int dk\,\exp(-2ikR)\chi(k)$, of the XAFS spectrum, k being the photoelectron wave number. Each path of total length L yields a peak in the Fourier transform near $L/2$. For fcc Cu metal, for example, the Fourier transform of the exact spectrum obtained by band-structure methods is observed to truncate beyond about six near-neighbor distances indicating that only path lengths less than about twelve near-neighbor distances are important for the entire spectrum.

This smearing effect can be described somewhat more picturesquely by considering a hypothetical series of calculations, where one calculates the density of states (DOS) of a solid (say copper) as a function of the path-length cutoff. As this cutoff is successively increased, more and more detail of the structure of the DOS appears, until, as one analytically sums to infinite order using the KKR equations, the ultimate degree of detail is revealed. Because various lifetime effects smear out the fine details of the structure, however, only a finite cutoff is required. This same cutoff governs the validity of cluster approaches to XAFS calculations. The size of the cluster needed to represent XAFS for an infinite solid is determined by the effective mean free path. Once clusters are bigger than a few mean free paths, the broadened results of cluster calculations converge to a fixed answer, independent of size, and hence only a finite-size cluster is required.

The main difference between cluster calculations and the path formalism is that an exact cluster approach is equivalent to carrying the path formalism to infinite order under the restriction that the paths only involve the atoms in the cluster (instead of all of the atoms in the infinite solid). Again, this difference is usually of little concern, provided the multiple-scattering expansion converges, since any additional fine details of a cluster calculation would be washed out by lifetime effects. It is, of course, possible that the multiple-scattering expansion will fail to converge, e.g., near resonances or singular points of the absorption spectrum. In those cases lifetime effects will still smear out sharp features of the spectrum, but some differences with respect to cluster or exact calculations may remain. The path method is thus complementary to exact or cluster methods in that convergence of the multiple-scattering expansion is implicitly assumed. This assumption can be checked, for example, by monitoring the convergence of the multiple-scattering expansion in the course of a calculation. Also, it may be possible in some cases to approximate resonances by analytically summing selected classes of paths to infinite order.

A straightforward, exact evaluation of the path formalism quickly runs into very complicated summations over angular momenta. As discussed in Ref. 5, each successive term involves an additional angular-momentum component (l,m) that must be added to the existing sums. Thus, single-scattering contributions require combining two angular momenta and hence a Wigner $3j$ symbol; double-scattering terms involve combining three angular momenta and $6j$ coefficients; triple scattering involves $9j$ coefficients and so on. To date the exact treatments have been limited to at most triple-scattering terms.[5] If one views the resulting complexity in terms of the number of l and m sums required, double scattering requires five l and six m sums and triple scattering seven l and five m sums. Moreover, $l_{\max}$ is usually large except at low energies; typically $l_{\max}\sim k_{\max}R_{mt}$ for XAFS studies is between 10 and 30 (R_{MT} is the muffin-tin radius). Although some standard angular-momentum identities can be used to eliminate some of these sums[5] (to five l and one m for double scattering and seven l and two m sums for triple scattering), it is clear that the algebraic complexity of the

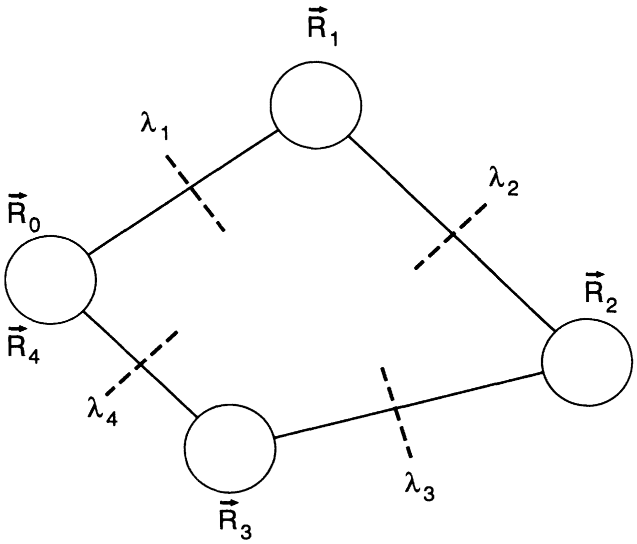

FIG. 1. Schematic four-leg multiple-scattering path with three scatterers. Each bond represents a Green's-function propagator, $G_{L,L'}(k(\mathbf{R}-\mathbf{R}'))$, and each node (except for node 0 = node 4) a scattering center. The dashed lines in the figure represent "cuts" that effectively separate each propagator into sums over the factors $\tilde{\Gamma}^{L}_{\lambda}(\rho)\Gamma^{L'}_{\lambda}(\rho)$ in the separable representation of Eq. (8).

formalism is so severe that only low-order terms are practical for XAFS calculations.

This straightforward but computationally demanding path expansion (or curved-wave theory) is in marked contrast with its asymptotic high-energy form. Then all of the outgoing spherical waves that the theory requires can be approximated by plane waves, yielding the plane-wave approximation[1] (PWA). This approximation completely eliminates all of the couplings between different partial waves and hence all the coupled l and m sums.

Within the PWA the contribution to the polarization-averaged K-shell XAFS spectrum $\chi^{(N-1)}(k)$ from a multiple-scattering path with N legs (i.e., $N-1$ scatterers) is given by a simple product over scattering amplitudes $f(\theta)$ in which the summation over angular momenta that is carried out at each site combines with the t matrices to produce ordinary scattering amplitudes. When the absorbing atom is at the origin $\mathbf{R}_0=\mathbf{R}_N$ and the scatterers at $\mathbf{R}_1,\mathbf{R}_2,\ldots,\mathbf{R}_{N-1}$ (Fig. 1), the N-leg contribution is given by

$$\chi^{(N-1)}(k)=\mathrm{Im}\left[\frac{e^{i(\rho_1+\rho_2+\cdots+\rho_N)+2i\delta_1}}{\rho_1\rho_2\cdots\rho_N}(\hat{\rho}_1\cdot\hat{\rho}_N)f_{N-1}(\theta_{N-1})\cdots f_2(\theta_2)f_1(\theta_1)\right] , \tag{1}$$

where k is the photoelectron wave number, $f_i(\theta_i)$ is the dimensionless plane-wave scattering amplitude at the ith scatterer, $\boldsymbol{\rho}_i=k(\mathbf{R}_{i+1}-\mathbf{R}_i)$ is the dimensionless bond vector, and $\theta_i=\cos^{-1}(\hat{\boldsymbol{\rho}}_i\cdot\hat{\boldsymbol{\rho}}_{i+1})$ is the scattering angle at site i. In terms of partial-wave phase shifts δ_l, the amplitude $f(\theta)$, which differs from the usual definition by a factor k, is given by

$$f(\theta)=\sum_l(2l+1)t_lP_l(\cos\theta) , \tag{2}$$

where $t_l=\exp(i\delta_l)\sin(\delta_l)$ is the dimensionless scattering t matrix, and $P_l(\cos\theta)$ is a Legendre polynomial of order l. The quantity in large parentheses in Eq. (1) is essentially the PWA for the contribution to the Green's function from this N-leg path; more precisely, $\chi^{(N-1)}(k)=\mathrm{Im}\{[e^{2i\delta_1}/(2l+1)]\sum_m G_{lm,lm}^{(N-1)}(\mathbf{R}_1,\ldots,\mathbf{R}_N)\}$. We will show that the multiple-scattering expansion for the Green's function, and hence $\chi^{(N-1)}(k)$, can be cast into the form of Eq. (1) *exactly*, provided the scattering amplitudes $f_i(\theta_i)$ are replaced by certain scattering matrices $F_{\lambda,\lambda'}$.

The simplicity of the plane-wave approach is obviously very desirable. Unfortunately, the validity of the PWA breaks down rapidly as one approaches the absorption edge, where curved-wave effects become increasingly important. For single scattering, one can go beyond the PWA and define effective scattering amplitudes that take spherical-wave effects into account exactly.[5-9] However, we believe this prescription cannot be generalized to multiple-scattering calculations of arbitrary path length. Perhaps the best one can do is to replace $f(\theta)$ in the PWA of Eq. (1) with effective curved-wave scattering amplitudes,[7]

$$\tilde{f}(\rho,\rho',\theta)=\sum_l(2l+1)t_lc_l(\rho)c_l(\rho')P_l(\cos\theta) . \tag{3}$$

This result is equivalent to the point-scattering approximation[1,10] (PSA) and is also obtained if one truncates the scattering matrices $F_{\lambda,\lambda'}$ to lowest order, i.e., to (1×1) matrices. Although quite good for nearly collinear paths and a significant improvement on the PWA, the PSA is not reliable at low energies for general θ (see, for example, Sec. IV B). It is for this reason that it is necessary to find a systematic method for going beyond both the PWA and PSA. In Eq. (3), $c_l(\rho)$ is the dimensionless polynomial factor that multiplies the asymptotic form of the spherical Hankel functions, i.e.,

$$h_l^{(+)}(\rho)=i^{-l}\frac{e^{i\rho}}{\rho}c_l(\rho) . \tag{4}$$

These "spherical-wave correction factors" play an important role in this paper. They may be generated efficiently by the Bessel function recurrence relation,

$$\begin{aligned} c_{l+1}(\rho)&=c_{l-1}(\rho)+(2l+1)\frac{i}{\rho}c_l(\rho) \quad (l>1) , \\ c_0(\rho)&=1,\quad c_1(\rho)=1+\frac{i}{\rho} . \end{aligned} \tag{5}$$

For large ρ one can show[7] that $c_l(\rho)\cong\exp[il(l+1)/2\rho][1+l(l+1)/2\rho^2]^{1/2}$. This implies that the PWA is valid in the limit $\rho\gg l(l+1)$, and also that the phase correction in $c_l(\rho)$ cannot be neglected in the intermediate energy range.[7] In these equations and throughout this paper it should be noted that we have adopted the phase conventions and notation of Messiah[11] for spherical Bessel functions, spherical harmonics, Legendre polynomials, and rotation matrices (see the Appendixes of Ref. 11).

The method we introduce here overcomes many of the difficulties of exact multiple-scattering calculations while retaining much of the simplicity and tractability of the PWA. With our approach, for example, a multiple-scattering expansion of the XAFS spectrum χ analogous to Eq. (1) is obtained, but with each scattering amplitude $f_i\ (\theta_i)$ replaced by a "scattering-amplitude matrix" (or "scattering matrix" for short) $F_{\lambda,\lambda'}(\rho,\rho')$. Also the method can be improved systematically by varying the dimensionality of the matrices, leading to generalized small-atom approximations. The lowest-order term is a (1×1) matrix or scalar function which is just the effective curved-wave scattering amplitude $\tilde{f}(\rho,\rho',\theta)$ of Eq. (3). Consequently, all of the PWA multiple-scattering formulas for XAFS, e.g., those used by Arvenitis *et al.*,[12] can be converted straightforwardly to exact curved-wave expressions, with a greater range of validity.

Our method is based on a new separable representation of the free Green's-function matrix elements $G_{L,L'}(\rho)=\langle L,\mathbf{R}|G|L',\mathbf{R}'\rangle$, where $\rho=k(\mathbf{R}-\mathbf{R}')$. These propagator (or translation operator) matrix elements $G_{L,L'}$ also appear in the addition formula for the translation of screened spherical waves[13–15] as well as in multiple-scattering expansions.[1–2,15] The theory of such functions has an extensive, if relatively obscure literature; a historical survey is given in Ref. 13. Like other researchers in this area, we have occasionally found some of our results in the literature only after having first worked them out independently by ourselves. However, we believe our approach is the first attempt at a direct separable representation of the propagator $G_{L,L'}$ and an elucidation of its properties.

The separable approximation, which becomes exact if summed over its full (finite) range of indices, is made possible by two steps: (1) successive rotations of the coordinate system that take bond directions $\hat{\rho}$ into the z axis; this step is similar to the strategy of Ref. 13 and yields results in terms of the simpler "z-axis propagators" $G_{L,L'}(\rho\hat{\mathbf{z}})$; and (2) a separable expansion in powers of $1/\rho$, analogous to a Taylor series, for the z-axis propagators. This multiple-scattering matrix formalism then permits independent summations at each site over all intermediate angular-momentum variables (l,m), as in the calculation of $f(\theta)$, thereby avoiding the computational bottleneck posed by large $l_{\max}$. We show below that this approach is rapidly convergent at all energies, leading to essentially exact results, provided the multiple-scattering expansion converges.

Somewhat analogous scattering matrices have been introduced in a multiple-scattering formulation by Barton and Shirley,[9] but our treatment differs from theirs in several respects, and they do not explicitly introduce a separable representation. We believe the present approach has better convergence and formal properties. For example, as noted above the dominant $[(1\times 1)$ matrix$]$ term in our expansion is the effective, spherical-wave scattering amplitude $f(\rho,\rho',\theta)$ defined in Eq. (3) and is symmetrical in ρ and ρ'. Thus our lowest-order approximation is equivalent to the asymptotic high-energy theory of Ref. 7 and to the point-scattering approximation of Refs. 1 and 10. By comparison, the zeroth-order term of the scattering matrices of Barton and Shirley is asymmetrical and independent of the magnitude of ρ'. Also, the form of our separable expansion leads to somewhat faster convergence of the remaining terms.

The remainder of this paper is organized as follows. The separable representation of the propagator is derived in Sec. II and applied to scattering matrices in Sec. III. Section IV contains applications to single- and double-scattering XAFS and single-scattering contributions in photoelectron diffraction. Details of the derivation of the separable representation are contained in two Appendixes. An application of this approach to a detailed treatment of multiple-scattering contributions in Cu is reserved for a separate paper.[16]

II. SEPARABLE REPRESENTATION OF THE PROPAGATOR

The multiple-scattering expansion for spherical scatterers is conveniently formulated in terms of (diagonal) scattering t matrices and matrix elements of the free propagator $G_{L,L'}(\rho)=\langle L,\mathbf{R}|G|L',\mathbf{R}'\rangle$ in an angular momentum $L=(l,m)$ and site basis $|L,\mathbf{R}\rangle$. Here, k is the wave number, which is related to the free-particle kinetic energy by $\varepsilon=\frac{1}{2}k^2$, and $\rho=k(\mathbf{R}-\mathbf{R}')$ denotes the dimensionless (bond) vector between two sites. Throughout this paper we will use hartree atomic units, $e=\hbar=m=1$. In this section we derive an exact separable representation of these matrix elements; they may be defined as the coefficients in the expansion in spherical waves of the dimensionless outgoing free propagator, $G(\mathbf{r},\mathbf{r}';\varepsilon)=-\exp(ik|\mathbf{r}-\mathbf{r}'|)/4\pi k|\mathbf{r}-\mathbf{r}'|$, about fixed sites $\mathbf{R}$ and $\mathbf{R}'$:

$$G(\mathbf{r},\mathbf{r}',\varepsilon)=\sum_{L,L'} j_L(\mathbf{r}-\mathbf{R})j^*_{L'}(\mathbf{r}'-\mathbf{R}')G_{L,L'}(\rho)\ . \qquad (6)$$

Here, $j_L(\mathbf{r})=i^l j_l(kr)Y_L(\hat{\mathbf{r}})$ are free spherical waves that are defined in terms of spherical Bessel functions $j_l(kr)$ and spherical harmonics $Y_L(\hat{\mathbf{r}})$, and $G_{L,L'}(\rho)$ is defined by the integral[17]

$$G_{L,L'}(\rho)=-\frac{(4\pi)^2}{2k}\int\frac{d^3k}{(2\pi)^3}\frac{Y^*_L(\hat{\mathbf{k}})Y_{L'}(\hat{\mathbf{k}})e^{i\mathbf{k}\cdot(\mathbf{R}-\mathbf{R}')}}{\varepsilon-\frac{1}{2}k^2+i0^+}\times\frac{j_l(kr)j_{l'}(kr')}{j_l(\sqrt{2\varepsilon}r)j_{l'}(\sqrt{2\varepsilon}r')}\ , \qquad (7)$$

where r and r' are arbitrary displacements. Equation (7) may be generalized for complex energies (i.e., inelastic losses) by adding an imaginary part to the energy: $\varepsilon+i0^+\rightarrow\varepsilon+i\Lambda$. With the normalization convention adopted above, $G_{L,L'}$ has the expansion in spherical waves given by[6] $G_{L,L'}(\rho)=4\pi\sum_{L''}\langle Y_L Y_{L''}|Y'_L\rangle h_{L''}(\mathbf{r})$, where $h_L(\mathbf{r})=i^l h_l^{(+)}(kr)Y_L(\hat{\mathbf{r}})$, and the t-matrix elements are dimensionless: $t_l=\exp(i\delta_l)\sin\delta_l$. The coefficients $G_{L,L'}$ also appear in the addition formula for the translation of spherical waves,[13–15] $h_L(\mathbf{r})=\sum_{L'}G_{L,L'}(k\mathbf{R})j_{L'}(\mathbf{r}-\mathbf{R})$.

The approach adopted in this paper for calculating $G_{L,L'}(\rho)$ is to seek a convergent separable representation, i.e., a representation of the form

$$G_{L,L'}(\rho)=\frac{e^{i\rho}}{\rho}\sum_{\lambda}\tilde{\Gamma}^{L}_{\lambda}(\rho)\Gamma^{L'}_{\lambda}(\rho)\ , \qquad (8)$$

where successive terms in λ are of decreasing significance, as discussed below. This is achieved in two steps.

(1) The first step is similar to that adopted in Ref. 13; one applies to Eq. (7) rotation matrices,[11] here denoted $R^l_{mm'}(\Omega_{\hat{\rho}})$, which rotate the bond direction $\hat{\rho}$ onto the z axis. More precisely, the argument $\Omega_{\hat{\rho}}$ represents the Euler angles for this rotation, namely, $(\alpha,\beta,\gamma)=(0,\theta,\pi-\phi)$, where (θ,ϕ) are the spherical polar coordinates of $\hat{\rho}$ (see footnote 1, p. 1073 of Ref. 11) and α is

set to zero. With this convention, the spherical harmonics transform as $Y_L(\hat{\mathbf{k}})=\sum_{m'}Y_{lm'}(\hat{\mathbf{k}}')R^l_{m'm}(\Omega_{\hat{\rho}})$, and $\hat{\mathbf{k}}'$ is along $\hat{\mathbf{z}}$ when $\hat{\mathbf{k}}$ is along $\hat{\boldsymbol{\rho}}$. These rotation operations separate $G_{L,L'}(\boldsymbol{\rho})$ exactly into energy-dependent radial and purely angular-dependent terms as follows:

$$G_{L,L'}(\boldsymbol{\rho})=\frac{e^{i\rho}}{\rho}\sum_{\mu=-l}^{l}R^l_{m\mu}(\Omega^{-1}_{\hat{\rho}})g^{(|\mu|)}_{ll'}(\rho)R^{l'}_{\mu m'}(\Omega_{\hat{\rho}}) , \qquad (9)$$

where $\Omega^{-1}_{\hat{\rho}}$ denotes the inverse rotation operation Euler angles $(\alpha,\beta,\gamma)^{-1}=(-\gamma,-\beta,-\alpha)=(\phi-\pi,-\theta,0)$, and $g^{(|\mu|)}_{ll'}(\rho)$ is a reduced, dimensionless, z-axis propagator given by

$$\begin{aligned}g^{(\mu)}_{ll'}(\rho)&=\rho e^{-i\rho}G_{l\mu,l'\mu}(\rho)\\ &=N_{l\mu}N_{l'\mu}\int_0^\infty\frac{dx}{z}e^{-x/z}P^\mu_l(1-x)P^\mu_{l'}(1-x) ,\\ &\qquad (\mu\geq 0) . \qquad (10)\end{aligned}$$

In Eq. (10), $N_{l\mu}=[(2l+1)(l-\mu)!/(l+\mu)!]^{1/2}$ are spherical-harmonic normalization factors, $z=1/i\rho$ ($i=\sqrt{-1}$), and $P^\mu_l(\cos\theta)$ are associated Legendre polynomials in $\cos\theta=(1-x)$. A derivation of Eq. (10) is presented in Appendix A. In this derivation only the outgoing wave is selected by the poles in Eq. (7) at $k=\pm(2\varepsilon+i0^+)^{1/2}$; the integration contour in Eq. (10) has been chosen to give only this outgoing part in a manner similar to that used in Eq. (29) of Ref. 13. The quantity $g^{(\mu)}_{ll'}(\rho)$ is similar to the spherical wave factor in the Hankel function analog $H^\mu_{ll'}(\rho)$ defined by Nozawa[14] in his Eq. (4.3); specifically $H^\mu_{ll'}(\rho)=(e^{i\rho}/\rho)g^{(\mu)}_{ll'}(\rho)/N_{l\mu}N_{l'\mu}$. Nozawa shows that an integral similar to Eq. (10) but over the range $-1\leq\cos\theta\leq 1$ gives the Bessel function analog $J^\mu_{ll'}(\rho)$; we find that changing the contour of Nazawa's integral to the range[14] $[i\infty,1]$ in $\cos\theta$ yields the outgoing part, which is Nozawa's function $H^\mu_{ll'}(\rho)$. The choice in Eq. (10) of the contour $[0,\infty]$ in x yields the same result, which can be verified by comparing series expansions. The introduction of rotation matrices and z-axis propagators simplifies considerably exact multiple-scattering calculations, since $G_{L,L'}(\rho\hat{\mathbf{z}})$ is then diagonal in m. This point has been emphasized both by Danos and Maximon[13] and by Barton and Shirley.[15] Moreover, we find that truncating the sum over μ yields accurate approximations; $\mu_{\max}\leq 2$ is usually sufficient. With step (1) alone, the summation of the multiple-scattering expansion requires only $l_{\max}\mu_{\max}$ intermediate terms at each site, rather than $l_{\max}(l_{\max}+1)$ terms in the exact case. While this reduction works well for paths with a small number of legs, it is still insufficient to make arbitrarily-high-order multiple-scattering calculations practicable, as successive l's are still coupled. The next step in the separation of $G_{L,L'}(\boldsymbol{\rho})$ overcomes this limitation.

(2) In the second step we derive a separable representation of the z-axis propagators. Specifically we find that one can express $g^{(\mu)}_{ll'}(\rho)$ as

$$g^{(\mu)}_{ll'}(\rho)=\sum_{\nu=0}^{\min\{l,\,l'-\mu\}}\tilde{\gamma}^l_{\mu\nu}(\rho)\gamma^{l'}_{\mu\nu}(\rho)\quad(\mu\geq 0) , \qquad (11)$$

where $\min\{l,l'\}$ denotes the minimum of l and l'. The details of this form are given in Appendix B. From Eq. (B10) the spherical expansion coefficients $\gamma^l_{\mu\nu}(\rho)$ and $\tilde{\gamma}^l_{\mu\nu}(\rho)$ are given, respectively, by series in inverse powers of ρ,

$$\begin{aligned}\gamma^l_{\mu\nu}(\rho)&=(-1)^\mu N_{l\mu}\frac{C_l^{(\mu+\nu)}(z)}{(\mu+\nu)!}z^{\mu+\nu} ,\\ \tilde{\gamma}^l_{\mu\nu}(\rho)&=\frac{(2l+1)}{N_{l\mu}}\frac{C_l^{(\nu)}(z)}{\nu!}z^\nu .\end{aligned}\qquad (12)$$

Here, $z=1/i\rho$, $C_l^{(\nu)}(z)=(d^\nu/dz^\nu)C_l(z)$ is a polynomial of degree $l-\nu$, and on changing variables from ρ to z, $C_l(z)$ is identical to $c_l(\rho)$, which is the degree-l polynomial factor of the spherical Hankel function in Eq. (4).

To examine convergence properties, we make use of the approximation $C_l(z)\sim\exp[-l(l+1)z/2]$ and find $C_l^{(\nu)}=O(l^{2\nu})$. Thus each term in the expansion in Eq. (11) converges roughly as $(l^2/\rho)^{2\nu+\mu}$. We remark that ρ is generally greater than unity even at the smallest bond lengths and energies above threshold, as the near-neighbor distance R_{nn} is always several atomic units and $k\geq k_F$, the Fermi momentum, which is of order unity in atomic units. Convergence with respect to l is controlled by the partial-wave t-matrix elements. The mean value of l suitably averaged over t_l, which we call $\bar{l}$, is characteristic of the "size" r_0 of the scatterer and is generally much smaller than $l_{\max}$. This maximum value of l may be defined as that for which the classical turning point is outside the range of the scattering potential, i.e., $l_{\max}(k)\sim kR_{\mathrm{MT}}$. For $l>l_{\max}$, δ_l becomes exponentially small. Provided $\bar{l}$ is sufficiently small, the expansion parameter $\bar{l}^2/\rho=(R_{\mathrm{MT}}/R)(\bar{l}^2/l_{\max})$ will also be small. While it is not evident this will always be the case, we have found in practice that it is usually sufficient to retain only the leading terms in Eq. (11), e.g., $\mu\leq 2$ and $\nu\leq 1$. Barton and Shirley[15] argue that the physical reason for the convergence of such expansions is that the higher "magnetic sublevels" μ have less overlap with the scattering potential; they also suggest that the number of sublevels needed for convergence is related to r_0/R. To see this one may picture $g^{(\mu)}_{ll'}$ as the overlap $\langle j_{l,\mu}(\mathbf{r}-R\hat{\mathbf{z}})|h_{l',\mu}(\mathbf{r})\rangle$ of an outgoing wave at the origin and a scattering state at $R\hat{\mathbf{z}}$; the outgoing wave has angular lobes at $\sin|\theta|\sim\mu/l'$ and the state $j_{l,\mu}$ has a mean radius of roughly $r_l\sim l/k$. Thus there is significant overlap only when $\mu<ll'/kR$. For scattering to be significant, $l<\bar{l}$ and hence $\mu<\bar{l}^2/kR$ which is just the small expansion parameter noted above. As a consequence, one can view truncations of the expansion in Eq. (11) as generalized small-atom approximations, which become increasingly better for smaller scatterers or larger k.

Given that the expansion parameter varies inversely with ρ, it is perhaps surprising that the truncated expansion is also accurate at low energies. The reason is that only a few partial waves are significant at low energies and all expansion coefficients $\gamma^l_{\mu\nu}$ must vanish for $|\mu|$, $\nu>l$. It follows that only the indices $|\mu|$, $\nu\leq l_{\max}(k)$ are important. The convergence of the multiple-scattering expansion with only a few terms (e.g., three to six) of the separable expansion is observed numerically to be valid at all energies.

For notational convenience we shall denote the expansion indices $(\mu\nu)$ by a single index λ. From Eqs. (8), (9), and (11), the explicit form of the factors $\Gamma_\lambda^L(\boldsymbol{\rho})$ and $\tilde{\Gamma}_\lambda^L(\boldsymbol{\rho})$ in $G_{L,L'}$ are

$$\tilde{\Gamma}_\lambda^L(\boldsymbol{\rho})=R_{m\mu}^{\,l}(\Omega_{\hat{\rho}}^{-1})\tilde{\gamma}_{\mu\nu}^{\,l}(\rho), \quad \Gamma_\lambda^L(\boldsymbol{\rho})=R_{\mu m}^{\,l}(\Omega_{\hat{\rho}})\gamma_{\mu\nu}^{\,l}(\rho) \; . \tag{13}$$

The separable representation in Eq. (8) with these coefficients is exact. Truncations at small $(\mu\nu)$ are accurate both at large energies or at large bond lengths (i.e., small $z=1/ikR$). Note that the lowest-order terms are $\tilde{\Gamma}_{00}^L=\sqrt{4\pi}Y_L^*(\theta,\phi)c_l(\rho)$ and $\Gamma_{00}^L=\sqrt{4\pi}Y_L(\theta,\phi)c_l(\rho)$. These terms are sufficient to obtain the point-scattering approximation, and in the limit $\rho\rightarrow\infty$ when $c_l(\rho)\rightarrow 1$, to recover the PWA.

III. SCATTERING-AMPLITUDE MATRICES

With the separable representation of $G_{L,L'}(\boldsymbol{\rho})$ developed above, the multiple-scattering expansion can be reexpressed in terms of scattering matrices. Consider for example the N path (Fig. 1) defined in Sec. I. The contribution to the total propagator from this path with $N-1$ scatterers is given by the exact multiple-scattering expansion

$$G_{L_N,L_0}^{(N-1)}(\mathbf{R}_1,\ldots,\mathbf{R}_N)=\sum_{\{L_i\}} G_{L_N,L_{N-1}}(\boldsymbol{\rho}_N)\cdots t_{l_2}(\mathbf{R}_2)G_{L_2,L_1}(\boldsymbol{\rho}_2)t_{l_1}(\mathbf{R}_1)G_{L_1,L_0}(\boldsymbol{\rho}_1) \; , \tag{14}$$

where L_0 and L_N denote fixed initial and final angular momenta. Substitution of the explicit expression for $G_{L,L'}(\rho)$ in Eq. (8) allows all the intermediate angular-momentum summations to be carried out formally. One can think of this process graphically in terms of the cuts introduced in the diagram in Fig. 1. The cuts, each of which is associated with an index λ, separate the left- and right-hand parts of $G_{L,L'}$ and isolate the intermediate vertex indices. One thus obtains the exact equivalent form

$$\begin{aligned}G_{L_N,L_0}^{(N-1)}(\mathbf{R}_1,\ldots,\mathbf{R}_N)=\frac{e^{(\rho_1+\rho_2+\cdots+\rho_N)}}{\rho_1\rho_2\cdots\rho_N}\sum_{\{\lambda_i\}} M_{\lambda_1,\lambda_N}^{L_0,L_N}(\boldsymbol{\rho}_1,\boldsymbol{\rho}_N)F_{\lambda_N,\lambda_{N-1}}(\boldsymbol{\rho}_N,\boldsymbol{\rho}_{N-1})\times\cdots\\ \times\cdots\times F_{\lambda_3,\lambda_2}(\boldsymbol{\rho}_3,\boldsymbol{\rho}_2)F_{\lambda_2,\lambda_1}(\boldsymbol{\rho}_2,\boldsymbol{\rho}_1) \; .\end{aligned} \tag{15}$$

Equation (15) is one of the principal results of this paper. It represents an exact formula for curved-wave multiple-scattering which is a direct analog of the PWA expression given by large parentheses in Eq. (1). In Eq. (15), the "scattering-amplitude matrices" $F_{\lambda\lambda'}(\boldsymbol{\rho},\boldsymbol{\rho}')$ at each site are defined by the partial wave expansion

$$\begin{aligned}F_{\lambda\lambda'}(\boldsymbol{\rho},\boldsymbol{\rho}')&=\sum_L t_l\Gamma_\lambda^L(\boldsymbol{\rho})\tilde{\Gamma}_{\lambda'}^L(\boldsymbol{\rho}')\\ &=\sum_l t_l\gamma_{\mu\nu}^{\,l}(\rho)R_{\mu\mu'}^{\,l}(\Omega_{\hat{\rho}\hat{\rho}'})\tilde{\gamma}_{\mu'\nu'}^{\,l}(\rho') \; ,\end{aligned} \tag{16}$$

where $\boldsymbol{\rho}$ and $\boldsymbol{\rho}'$ are the bonds leading to and from the site in question. The separable angular-momentum-dependent termination matrix in Eq. (16) is

$$M_{\lambda_0,\lambda_N}^{L_0,L_N}(\boldsymbol{\rho}_1,\boldsymbol{\rho}_N)=\Gamma_{\lambda_0}^{L_0}(\rho_1)\tilde{\Gamma}_{\lambda_N}^{L_N}(\rho_N) \; . \tag{17}$$

This expression can often be simplified, e.g., when $L_0=L_N$; see Sec. IV A.

The composite rotation matrix $R_{\mu\mu'}^{\,l}(\Omega_{\hat{\rho}\hat{\rho}'})$ in Eq. (16) is equivalent to a rotation that first takes $\hat{\boldsymbol{\rho}}$ into $\hat{\mathbf{z}}$ and then $\hat{\mathbf{z}}$ into $\hat{\boldsymbol{\rho}}'$. Replacing the scattering angle in the PWA formula are the Euler angles corresponding to this bond rotation, $(\alpha,\beta,\gamma)\equiv\Omega_{\hat{\rho}\hat{\rho}'}$; they may be obtained by an explicit construction of the composite rotation matrix, for say $l=1$,

$$R_{\mu\mu'}^{\,l}(\Omega_{\hat{\rho}\hat{\rho}'})=\sum_{m''}R_{mm''}^{\,l}(0,\theta,\pi-\phi)R_{m''m'}^{\,l}(\phi'-\pi,-\theta',0) \; ,$$

using Eq. (C.56) and (C.75) of Ref. 11. We obtain

$$\begin{aligned}\alpha&=\arg[\sin\theta\cos\theta'-\cos\theta\sin\theta'\cos(\phi'-\phi)\\ &\qquad -i\,\sin\theta'\sin(\phi'-\phi)] \; ,\\ \beta&=\cos^{-1}(\hat{\boldsymbol{\rho}}\cdot\hat{\boldsymbol{\rho}}')\\ &=\cos^{-1}[\cos\theta\cos\theta'+\sin\theta\sin\theta'\cos(\phi-\phi')] \; ,\\ \gamma&=\arg[\sin\theta\cos\theta'\cos(\phi'-\phi)-\cos\theta\sin\theta'\\ &\qquad +i\,\sin\theta\sin(\phi'-\phi)] \; .\end{aligned} \tag{18}$$

Note that these Euler angles depend only on three physical angles: θ, θ', and $\phi-\phi'$; they may also be calculated in terms of the direction cosines of the vectors $\hat{\boldsymbol{\rho}}$ and $\hat{\boldsymbol{\rho}}'$. Since the rotation matrices can be factored as $R_{\mu\mu'}^{\,l}(\alpha,\beta,\gamma)=\exp(-i\alpha\mu)r_{\mu\mu'}^{\,l}(\beta)\exp(-i\gamma\mu')$, the scattering matrices can be expressed similarly,

$$F_{\lambda,\lambda'}(\boldsymbol{\rho},\boldsymbol{\rho}')=e^{-i\alpha\mu}f_{\lambda,\lambda'}(\rho,\rho',\beta)e^{-i\gamma\mu'} \; . \tag{19}$$

Thus the energy-dependent scattering factors $f_{\lambda,\lambda'}(\rho,\rho',\beta)$ now depend only on the bond lengths and the scattering angle β [which is equivalent to $\theta=\cos^{-1}(\hat{\boldsymbol{\rho}}\cdot\hat{\boldsymbol{\rho}}')$],

$$f_{\lambda,\lambda'}(\rho,\rho',\beta)=\sum_l t_l\gamma_{\mu\nu}^{\,l}(\rho)r_{\mu\mu'}^{\,l}(\beta)\tilde{\gamma}_{\mu'\nu'}^{\,l}(\rho') \; . \tag{20}$$

This form considerably reduces the number of independent computations of the scattering matrices. Furthermore the only additional angle needed in the calculations is the combination $\eta_i = \gamma_i + \alpha_{i+1}$ at each scattering site i. For comparison, the point-scattering approximation requires bond lengths ρ_i and scattering angles β_i, and the PWA only the scattering angles β_i.

The dependence of the coefficients $\tilde{\gamma}^l_{\mu\nu}(\rho)$ and $\gamma^l_{\mu\nu}(\rho)$ on ρ implies that $F_{\lambda\lambda'}(\boldsymbol{\rho},\boldsymbol{\rho}') \sim (\rho)^{-(2\nu+\mu)}(\rho')^{-(2\nu'+\mu')}$ for large ρ,ρ', and hence, the dominant matrix element is generally $F_{00,00}$. This is precisely the effective, curved-wave scattering amplitude $F_{00,00}(\boldsymbol{\rho},\boldsymbol{\rho}') = f_{00,00}(\rho,\rho',\beta) = \tilde{f}(\rho,\rho',\beta)$ as defined in Eqs. (16), (20), and (3), respectively. Keeping only this dominant term is equivalent to the point-scattering approximation, and yields contributions to XAFS as in Eq. (1), but with the effective scattering amplitudes $\tilde{f}(\rho,\rho',\beta)$ replacing $f(\theta)$, as we have noted in the Introduction. The next level of approximation consists of keeping all terms up to first order in $1/\rho$. This yields a (3×3) matrix containing only the terms $(\mu\nu) = (0,0),(\pm1,0)$. The second-order expression correct to $O(1/\rho^2)$ is a (6×6) matrix that, in addition, contains the terms $(0,1)$ and $(\pm2,0)$. In practice it seems sufficient to retain terms only to second order. These approximations will be tested in the next section.

IV. APPLICATIONS

A. Single-scattering polarized and unpolarized XAFS

As a simple application we apply this formalism to the normalized single-scattering XAFS amplitude for a polycrystalline material. One obtains[1,4,6] for the contribution from a given subshell l

$$\chi_l^{(1)}(k) = \mathrm{Im}\, e^{2i\delta_l} \frac{1}{2l+1} \sum_m G^{(1)}_{lm,lm}(\mathbf{R}_1,\mathbf{R}_2) \;, \tag{21}$$

where $G^{(1)}_{lm,lm}(\mathbf{R}_1,\mathbf{R}_2)$ is given by Eq. (14). Note that for $L_0 = L_N$ in Eq. (14), the form of termination matrix simplifies upon carrying out the trace over m. One then obtains a result similar to Eq. (15), but with the matrix $M^{L_0,L_N}_{\lambda_1,\lambda_0}$ replaced by a form incorporating a composite rotation matrix:

$$M^l_{\lambda_1,\lambda_N}(\boldsymbol{\rho}_1,\boldsymbol{\rho}_N) = \gamma^l_{\mu\nu}(\rho_1) R^l_{\mu\mu'}(\Omega_{\hat{\rho}_1\hat{\rho}_N}) \tilde{\gamma}^l_{\mu'\nu'}(\rho_N) \;. \tag{22}$$

By inspection $M^l_{\lambda,\lambda'}(\boldsymbol{\rho},\boldsymbol{\rho}')$ is the lth term in the partial-wave formula of Eq. (16) for the scattering matrix $F_{\lambda,\lambda'}(\boldsymbol{\rho},\boldsymbol{\rho}')$, and may thus be calculated with the same subroutine.

In the present case of single-scattering XAFS the composite rotation corresponds to the inversion $\hat{\mathbf{R}} \to -\hat{\mathbf{R}}$, for which the rotation matrix is diagonal: $R^l_{\mu\mu'} = (-1)^l \delta_{\mu,\mu'}$. Hence we obtain

$$\chi_l^{(1)}(k) = -\mathrm{Im} \frac{e^{2i\rho+2i\delta_l}}{\rho^2} \frac{1}{2l+1} \times \left(\sum_{\mu=-l}^{l} \sum_{\nu,\nu'=0}^{l} \gamma^l_{\mu\nu}(\rho) \tilde{\gamma}^l_{\mu\nu'}(\rho) f_{\mu\nu,\mu\nu'}(\rho,\rho,\pi) \right) , \tag{23}$$

where $f_{\mu\nu,\mu\nu'}(\rho,\rho,\pi) = \sum_l (-1)^l t_l \gamma^l_{\mu\nu}(\rho) \tilde{\gamma}^l_{\mu\nu'}(\rho)$. The term in large parentheses may be interpreted as an l-shell effective back-scattering amplitude $\tilde{f}_l(\rho,\pi)$. From the form of the factors $\gamma^l_{\mu\nu}$, one can show explicitly that the quantity in large parentheses in Eq. (23) with $l=1$ is equal to the exact K-shell, single-scattering, curved-wave formula of Müller and Schaich.[6] We remark that Eq. (23) may be useful in obtaining the contribution to the unpolarized XAFS from an arbitrary core level. Similarly, Eq. (15) may be useful for the polarized case [see, for example, Eq. (A16) of Ref. 1], as all the algebra special to a given shell is automatically incorporated in the termination matrix $M^{L,L'}_{\lambda,\lambda'}$ of Eq. (15).

B. Double-scattering XAFS

An important test of the method is the calculation of multiple scattering in fcc Cu, which is an oft-used standard test case for XAFS theories. This metal has mostly weak scattering in the first 50 eV above the edge, which is one reason why it is often considered a free-electron-like material in terms of its low-energy excitations. However, the scattering strength begins to turn on strongly between 50 to 500 eV (k between 4 and 10 Å^{-1}) as the energy goes through the $4d$, $4f$, and other resonances. This is clearly seen in the back-scattering amplitude as a function of energy or k [see Fig. 1(a) of Ref. 7(a) and the discussion of the electronic structure of Cu in Ref. 4(b)]. Thus Cu exhibits the full range of XAFS behavior as a function of energy. At low energies above the edge, only the single-scattering terms in the path formalism are required for convergence. At higher energies a complete treatment of multiple-scattering is required. Figure 2 of Ref. 7(a) clearly shows the failure of single-scattering and shadowing terms between 50 and 200 eV above the edge.

Therefore, we have applied our method to the contribution from all relevant triangular (double-scattering) paths to the K-shell XAFS of Cu metal. We have also included this application because triangular paths are sufficiently high order to be nontrivial, and tractable exact formulas can also be used for precise comparisons.[3] For this case, the multiple-scattering contribution to $\chi^{(2)}$ analogous to Eq. (23) is

$$\chi_l^{(2)}(k) = \mathrm{Im} \frac{e^{i(\rho_1+\rho_2+\rho_3)+2i\delta_1}}{\rho_1\rho_2\rho_3} \times \tfrac{1}{3} \sum_{\{\lambda_l\}} M^l_{\lambda_1,\lambda_3}(\boldsymbol{\rho}_1,\boldsymbol{\rho}_3) F_{\lambda_3,\lambda_2}(\boldsymbol{\rho}_3,\boldsymbol{\rho}_2) \times F_{\lambda_2,\lambda_1}(\boldsymbol{\rho}_2,\boldsymbol{\rho}_1) \;, \tag{24}$$

where $M^l_{\lambda,\lambda'}$ is given by Eq. (22).

The necessary ingredients in the calculation of $F_{\lambda,\lambda'}$ and $M^l_{\lambda,\lambda'}$ are (a) the geometry-dependent rotation matrix elements $r^l_{m,m'}(\beta)$, where β is the scattering angle (α and γ are zero since the scattering vectors lie in a plane); (b) the energy-dependent scattering t-matrix elements; and (c) the spherical-wave factors $\gamma^l_{\mu\nu}(\rho)$ and $\tilde{\gamma}^l_{\mu\nu}(\rho)$. The rotation matrix elements were calculated by recursion, using an iterated version of Eq. (4.4.1) of Ref. 18. The energy-dependent factors were also obtained by recur-

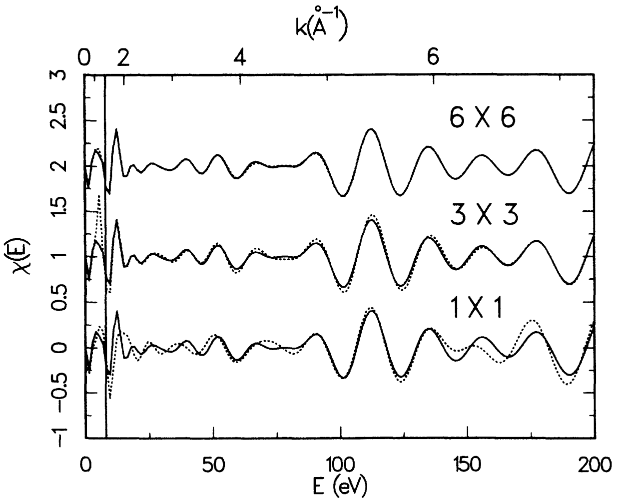

FIG. 2. Contribution to the K-shell XAFS spectrum of fcc Cu from 107 topologically distinct angular multiple-scattering paths, with a total path length less than six near-neighbor (NN) distances ($R_{\text{NN}}=4.80$). Each of these distinct paths represent between 12 and 48 symmetry-related degenerate paths that give identical contributions to $\chi(E)$. The dashed curves are, respectively, results from (1×1), (3×3), and (6×6) scattering matrices. For reference, the exact results are superimposed on each of these curves as a solid line. The energy scale is relative to the band-structure muffin-tin zero [Ref. 4(b)] and the solid vertical line at 7.9 eV is the band-structure Fermi energy E_F. The $\chi(E)$ for each of the plots is reduced by a factor of 4 below E_F to keep the different plots from overlapping each other.

sion, using Eq. (B9) of the Appendix. Finally the t-matrix elements were those obtained by calculating the partial-wave phase shifts from self-consistent band-structure potentials, and are the same as those used in Ref. 4.

Calculations based on Eq. (24) were then carried out summing over all 107 topologically distinct triangular paths with a total path length less than six near-neighbor distances using 10 phase shifts and 100 points in the energy range from 0 to 200 eV. The results are shown in Fig. 2 for zeroth-order (1×1) matrices, first-order (3×3), and second-order (6×6) matrix approximations. For comparison, the results of exact calculations based on Eq. (21) of Ref. 3 are also presented. Note that the zeroth-order calculation is already in fair agreement with the exact results, and that the result for (6×6) matrices is nearly converged. The approximate run times on a Cray Research, Inc. X-MP supercomputer at Los Alamos are 5, 11, 29, and 60 central-processing-unit (CPU) sec for zeroth, first, and second order, and exact calculations, respectively. Thus the method is indeed rapidly convergent and accurate down to the edge.

On the basis of these results we may estimate that a triple-scattering calculation with the separable approximation will require an additional factor of about 6 per path, which is a significant improvement over the factor of $O(l_{\max}^2)\sim100$ required for exact calculations. Finally we note that the magnitude $|\chi_l^{(N)}(k)/\chi_l^{(1)}(k)|$ summed over intermediate paths, can also be used as a convergence monitor of the multiple-scattering expansion.

C. Single-scattering photoelectron diffraction

The separable curved-wave multiple-scattering formalism presented here is applicable to many other spectroscopies that depend on the final state of the photoelectron. For example, for the case of photoelectron diffraction, the intensity at the detector is[19,20]

$$\frac{d\sigma}{d\Omega}\propto\left|\sum_{L,N}G_{00,L}^{(N-1)}(\mathbf{R}_1,\ldots,\mathbf{R}_N)m_{L,c}(\hat{\boldsymbol{\varepsilon}})e^{i\delta_l^c}\right|^2, \tag{25}$$

where the Green's function is given by Eq. (14), $m_{Lc}(\hat{\boldsymbol{\varepsilon}})=\langle\psi_L(k)|\hat{\boldsymbol{\varepsilon}}\cdot\mathbf{r}|\psi_{Lc}\rangle$ is the dipole matrix element, and the sum is over the N-leg paths, $\mathbf{R}_\infty=\mathbf{R}_N$, $\mathbf{R}_{N-1},\ldots,\mathbf{0}$, $N=1,2,\ldots$, where $\mathbf{R}_\infty=\hat{\mathbf{k}}R_\infty$ is the vector to the detector. For a degenerate core level, an average over initial states ψ_{Lc} must also be carried out. Since the detector distance can be assumed to be infinite, only $\gamma_{0,0}^l(\infty)=\sqrt{2l+1}$ and $\tilde{\gamma}_{\mu0}^l(\infty)=\sqrt{2l+1}$ are nonzero, so that the expressions simplify. For the direct ($N=1$) and single-scattering ($N=2$) terms, one obtains

$$\frac{d\sigma}{d\Omega}\propto\left|\sum_L m_{L,c}(\hat{\boldsymbol{\varepsilon}})e^{i\delta_l^c}\left[Y_L(\hat{\mathbf{k}})+\frac{e^{ikR(1-\cos\theta)}}{R}\sum_\lambda F_{00,\lambda}(\boldsymbol{\rho}_\infty,\boldsymbol{\rho})M_{\lambda,00}^{L,00}(\boldsymbol{\rho},\boldsymbol{\rho}_\infty)\right]\right|^2, \tag{26}$$

where the terms in the sum over λ are defined in Eqs. (15)–(19). This sum can be interpreted as the effective curved-wave single-scattering amplitude. Equation (26) is formally equivalent to the cumbersome exact formulas of Ref. 20 and, moreover, can be applied to an arbitrary core level.

ACKNOWLEDGMENTS

We gratefully acknowledge stimulating discussions with J. J. Barton concerning separable approximations. We also thank C. S. Fadley, R. Felton, and E. A. Stern for comments, and especially J. Mustre de Leon for helpful suggestions and programming assistance. One of us (J.J.R.) acknowledges the hospitality of the Laboratory of Atomic and Solid State Physics at Cornell University, where part of this work was carried out during a sabbatical leave. This work was also supported in part by U.S. Department of Energy (DOE) Contract No. W-7405-Eng-36 (RCA).

APPENDIX A

In this Appendix we present a derivation of the reduced, dimensionless, z-axis propagator given by Eq. (10). Our starting point is the conventional definition of the

Green's function: $G^+(\mathbf{r},\mathbf{r}';\varepsilon)\equiv\langle\mathbf{r}|(\varepsilon-H+i0^+)^{-1}|\mathbf{r}'\rangle$, where $H=-\hbar^2\nabla^2/2m$. The Green's function actually used in this paper is $G=-G^+/\xi$, where the factor $\xi=(2m/\hbar^2)(2m\varepsilon/\hbar^2)^{1/2}$. In the atomic hartree units ($e=\hbar=m=1$) used in this paper, $\xi=2k$, where $k=\sqrt{2\varepsilon}$. The advantage of this notation [where we follow Schaich, Ref. 6(b)] is to make the Green's function dimensionless as well as to remove an annoying minus sign in the final reduced form for G. Furthermore, since the inverse of this same factor ξ occurs in the t matrix, our t matrix [see the definition just below Eq. (2)], which is the conventional t matrix multiplied by ξ, is then also dimensionless. With these choices the product of Gt that naturally occurs in the multiple-scattering expansion [see Eq. (14)] remains invariant while allowing for dimensionless G's and t's. Equations (9) and (10) of Ref. 2 show the factors of ξ in G and t in a particularly transparent fashion.

By inserting a complete set of plane-wave states on either end of $(\varepsilon-H+i0^+)^{-1}$, we can write the dimensionless Green's function in atomic hartree units as

$$G(\mathbf{r},\mathbf{r}';\varepsilon)=-\frac{1}{2\sqrt{2\varepsilon}}\int\frac{d^3k}{(2\pi)^3}\frac{e^{i\mathbf{k}\cdot(\mathbf{r}-\mathbf{r}')}}{\varepsilon-\frac{1}{2}k^2+i0^+}\ . \tag{A1}$$

If we then rewrite

$$e^{i\mathbf{k}\cdot(\mathbf{r}-\mathbf{r}')}=e^{i\mathbf{k}\cdot(\mathbf{r}-\mathbf{R})}e^{i\mathbf{k}\cdot(\mathbf{R}-\mathbf{R}')}e^{i\mathbf{k}\cdot(\mathbf{r}'-\mathbf{R}')}\ , \tag{A2}$$

expand the first and last exponentials on the right-hand side into spherical harmonics and Bessel functions [Eq. (B.105), p. 497, of Ref. 11], and rewrite Eq. (A1) in the form of Eq. (6) to pick off $G_{L,L'}(\rho)$, we obtain Eq. (7).

We now need to manipulate the radial integral over $\int dk\,k^2$ so that it extends from $-\infty$ to ∞. To do this we make two transformations that take advantage of the symmetries: $Y_L(-\hat{\mathbf{k}})=(-1)^l Y_L(\hat{\mathbf{k}})$ and $j_l(-\rho)=(-1)^l j_l(\rho)$. The first transformation is $\hat{\mathbf{k}}\rightarrow-\hat{\mathbf{k}}$. This changes Eq. (7) by a factor of $(-1)^{l+l'}$ from the spherical harmonics symmetry and changes the sign of the exponential argument. The second transformation is to change variables in the radial k integral from $k\rightarrow-k$. If we ignore the angular integral and other factors to focus on this integral alone, we find from the Bessel function symmetry

$$\int_0^\infty dk\,k^2\frac{e^{ik\hat{\mathbf{k}}\cdot(\mathbf{r}-\mathbf{r}')}j_l(kr)j_{l'}(kr')}{\varepsilon-\frac{1}{2}k^2+i0^+}=(-1)^{l+l'}\int_{-\infty}^0 dk\,k^2e^{ik\hat{\mathbf{k}}\cdot(\mathbf{r}-\mathbf{r}')}\frac{j_l(kr)j_{l'}(kr')}{\varepsilon-\frac{1}{2}k^2+i0^+}\ . \tag{A3}$$

Combining the two transformations explicitly demonstrates that the expression for G with the radial k integral from $-\infty$ to 0 is identical to that from 0 to ∞ and allows us to write

$$G_{L,L'}=-\frac{1}{2}\frac{(4\pi)^2}{2\sqrt{2\varepsilon}}\int\frac{d\hat{\mathbf{k}}}{(2\pi)^3}\int_{-\infty}^{\infty}dk\,k^2\frac{Y_L^*(\hat{\mathbf{k}})Y_{L'}(\hat{\mathbf{k}})e^{i\mathbf{k}\cdot(\mathbf{R}-\mathbf{R}')}}{\varepsilon-\frac{1}{2}k^2+i0^+}\frac{j_l(kr)j_{l'}(kr')}{j_l(\sqrt{2\varepsilon}r)j_{l'}(\sqrt{2\varepsilon}r')}\ . \tag{A4}$$

The prefactor of $\frac{1}{2}$ takes care of the double counting caused by extending the radial k integral to $-\infty$. To finish the derivation of Eq. (10) we now specialize to the coordinate system where $\mathbf{R}-\mathbf{R}'$ is along the $\hat{\mathbf{z}}$ direction. Then $\hat{\mathbf{k}}\cdot(\mathbf{r}-\mathbf{r}')=\mu|\mathbf{r}-\mathbf{r}'|$, where $\mu\equiv\cos\theta$,

$$Y_L(\hat{\mathbf{k}})=\frac{(-1)^m}{\sqrt{4\pi}}N_{lm}P_l^m(\mu)e^{im\phi},\quad m>0 \tag{A5}$$

and, since $Y_{lm}^*(\hat{\mathbf{k}})=(-1)^m Y_{l,-m}(\hat{\mathbf{k}})$, the factor of $(-1)^m$ is missing in Eq. (A5) for $m<0$ (and $m\rightarrow|m|$ everywhere in the equation. The normalization factor N_{lm} is given just below Eq. (10) in the text, where the associated Legendre polynomials P_l^m are also defined. If we make these substitutions, the integral over ϕ gives $2\pi\delta_{m,m'}$ and the integral over k can be done by contour integration (closing in the upper half plane for $\mu>0$ and in the lower-half plane for $\mu<0$). The same result occurs for both positive and negative m if we substitute $|m|$ for m everywhere in all subsequent formulas in this Appendix. In this specialized coordinate system we then have

$$G_{L,L'}(\rho)=\delta_{m,m'}N_{lm}N_{l'm}\left[\frac{i}{2}\right]\times\int_{-1}^{1}d\mu\,\tilde{E}(\mu)P_l^m(\mu)P_{l'}^m(\mu)\ , \tag{A6}$$

where

$$\tilde{E}(\mu)=\begin{cases}e^{i\rho\mu} & \text{for } \mu>0\ ,\\ (-1)^{l+l'}e^{-i\rho\mu} & \text{for } \mu>0\ ,\end{cases} \tag{A7}$$

and $\rho=\sqrt{2\varepsilon}|\mathbf{R}-\mathbf{R}'|$. We can then use the symmetry $P_l^m(-\mu)=(-1)^{l-m}P_l^m(\mu)$ to show that the integral from -1 to 0 is equal to that from 0 to 1. After removing the factor of $e^{i\rho}/\rho$ and changing variables to $x=1-\mu$ and $z=1/i\rho$, we then obtain Eq. (10), except that the integral over x goes from 0 to 1. We have been able to show, in analogy to the procedures used in Ref. 13, that the integral over the same integrand from 1 to ∞ in x vanishes, which enables us to write Eq. (10) with the integral extending from 0 to ∞, as written.

APPENDIX B

Here we present a derivation of the separable representation of Eq. (11) using contour integration techniques. The derivation is based on an identity relating the Laplace transform of a product $a(x)b(x)$ to a "double Taylor series." A brief derivation is as follows. Define the product transform $I(z)$ as

$$I(z)=\int_0^\infty \frac{dx}{z}a(x)b(x)e^{-x/z}$$
$$=\int_C \frac{dz_1}{2\pi i}\int_C \frac{dz_2}{2\pi i}\,\frac{A(z_1)B(z_2)}{z_1z_2-zz_2-zz_1}\ , \tag{B1}$$

where we have substituted the inverse transforms

$$a(x)=\int_C \frac{dz}{2\pi i}\,\frac{A(z)}{z}e^{x/z},\quad b(x)=\int_C \frac{dz}{2\pi i}\,\frac{B(z)}{z}e^{x/z}\ , \tag{B2}$$

and the contour C is to the right of poles of $A(z)$ and $B(z)$. The transform $A(z)$ is given by Eq. (B1) with $b(x)=1$. If $a(x)$ has a Taylor series expansion about the origin, $a(x)=\sum_{n=0}a_nx^n$, the Taylor expansion of $A(z)$ is $A(z)=\sum_{n=0}n!a_nz^n$. Carrying out the integration over z_2 in Eq. (B1) yields

$$I(z)=\int_C \frac{dz_1}{2\pi i}\,\frac{A(z_1)B[z_2(z_1)]}{z_1-z}\ ,$$
$$z_2(z_1)=z+\frac{z^2}{z_1-z}=\frac{zz_1}{z_1-z}\ . \tag{B3}$$

Substituting Taylor expansions for A and B about z, i.e., $A(z')=\sum_n A^{(n)}(z)(z'-z)^n/n!$, where $A^{(n)}$ is the nth derivative of $A(z)$, and noting that only simple poles survive the integration then yields

$$I(z)=\sum_{n=0}^{\infty}\frac{A^{(n)}(z)}{n!}\,\frac{B^{(n)}(z)}{n!}z^{2n}\ , \tag{B4}$$

which we have termed a double Taylor series in analogy with its functional form.

For the case of Eq. (10) this formula is simplest to apply when $m=0$, in which case one obtains

$$g_{ll'}^{(0)}(\rho)=\int_0^\infty \frac{dx}{z}P_l(1-x)P_{l'}(1-x)$$
$$=\sum_{n=0}^{\min\{l,l'\}}\frac{C_l^{(n)}(z)}{n!}\,\frac{C_{l'}^{(n)}(z)}{n!}z^{2n}\ . \tag{B5}$$

For the general case $m\neq0$ in Eq. (10) the associated Legendre polynomials $P_l^m\propto(\sin\theta)^{m/2}P_l^{(m)}$ each have a factor $(\sin\theta)^{m/2}=(2x-x^2)^{m/2}$, and hence are not finite polynomials in x for odd m. For this reason we find it convenient to associate both of these prefactors with the first $P_l^{(m)}$ factor in the integrand, which results in an asymmetrical form for $m\neq0$, but yields finite polynomial expansions for all m. Thus in Eq. (B1) we define

$$a(x)=(2x-x^2)^mP_l^{(m)}(1-x)$$
$$=\frac{1}{(2m-1)!!}P_m^m(1-x)P_l^m(1-x)\ , \tag{B6}$$
$$b(x)=P_{l'}^{(m)}(1-x)\ . \tag{B7}$$

The transform $A(z)$ can be evaluated with the help of Nozawa's Eq. (6.1) for $n=m$ and the correspondence discussed below Eq. (10) between $H_{ll'}^m$ and integrals of the form of Eq. (10). The transform of $a(x)$ chosen above corresponds to the function $H_{lm}^m(\rho)$, and we obtain

$$H_{lm}^m(\rho)=\frac{e^{i\rho}}{\rho}\,(2m-1)!!\,A(z)$$
$$=\frac{e^{i\rho}}{\rho}z^m\,(2m-1)!!\,C_l(z)\frac{(l+m)!}{(l-m)!}\ , \tag{B8}$$

so that $A(z)=[(l+m)!/(l-m)!]z^mC_l(z)$. The transform $B(z)$ can be obtained directly from the Taylor series expansion of $C_l(z)$ as follows: $B(z)=(-1)^m\sum_{n=0}^{l'-m}p_{l',n+m}z^n$, where $p_{l,n}=(-1)^n(l+n)!/(l-n)!(2n)!!$ are the coefficients of $C_l(z)=\sum_{n=0}^{l}p_{l,n}z^n$. Hence we obtain for the integrand in Eq. (B3)

$$A(z_1)B[z_2(z_1)]=(-1)^m\frac{(l+m)!}{(l-m)!}(z+\delta)^mC_l(z+\delta)$$
$$\times\sum_{n=0}^{l'-m}p_{l',n+m}(z+z^2/\delta)^n$$
$$=(-1)^m\frac{(l+m)!}{(l-m)!}\,\frac{\delta^m}{z^m}C_l(z+\delta)$$
$$\times\widetilde{C}_{l'}(z+z^2/\delta)\ , \tag{B9}$$

where $\delta=z_1-z$. In arriving at the last line of Eq. (B9) we have rewritten $(z+z^2/\delta)^n=(z/\delta)^n(z+\delta)^n$ and combined terms. The quantity $\widetilde{C}_l=\sum_{n=m}^{l}p_{l,n}z^n$ has the same Taylor expansion as $C_l(z)$ beyond the mth term. Instead of carrying out the derivatives of $A(z)$ and $B(z)$ as in Eq. (B4), it is simpler to redo the contour integration in Eq. (B3) with the above integrand. Substituting Eq. (B9) into (B2), again noting that the integration only counts the single pole terms, then gives

$$\int_0^\infty \frac{dx}{z}e^{-x/z}P_l^\mu(1-x)P_{l'}^\mu(1-x)=\frac{(l+m)!}{(l-m)!}\sum_{n=0}^{\min\{l,\,l'-m\}}(-1)^m\frac{C_l^{(n)}(z)}{n!}\,\frac{C_{l'}^{(n+m)}(z)}{(n+m)!}z^{2n+m}\ , \tag{B10}$$

where $C_l^{(m)}(z)=d^mC_l(z)/dz^m$. Note that the overtilde is not necessary in the term in $C_{l'}^{(n+m)}(z)$ by virtue of their common Taylor expansions beyond the mth term.

The quantities $C_l^{(m)}(z)$ can be computed efficiently at each energy from recursion relations in terms of an auxiliary function $C_{lm}(z)=C_l^{(m)}z^m/m!$. By differentiating the recurrence relation $d^m/dz^m[C_{l+1}=C_{l-1}-(2l+1)zC_l]$, one finds that

$$C_{l+1,m}=C_{l-1,m}-(2l+1)z(C_{l,m}+C_{l,m-1}) ,$$
$$C_{m,m}=(-1)^m\frac{(2m)!z^m}{2^m m!} \tag{B11}$$

(arguments suppressed), where the quantity $C_{m,m}$ is obtained from the Taylor expansion coefficients of $C_l(z)$ given above. Because the coefficients $C_{lm}(z)$ depend on bond length via the factors $C_l^{(m)}(z)$, their dependence on $\rho=kR$ is due primarily to a shift in the phase of order $l(l+1)/\rho$ and an amplitude factor of order ρ^{-m}.

---

[1] P. A. Lee and J. B. Pendry, Phys. Rev. B **11**, 2795 (1975).

[2] W. L. Schaich, Phys. Rev. B **8**, 4028 (1973); C. A. Ashley and S. Doniach, *ibid.* **11**, 1279 (1975).

[3] P. J. Durham, J. B. Pendry, and C. H. Hodges, Comput. Phys. Commun. **25**, 193 (1982).

[4] (a) J. E. Müller and J. W. Wilkins, Phys. Rev. B **29**, 4331 (1984); (b) R. C. Albers, A. K. McMahan, and J. E. Müller, *ibid.* **31**, 3435 (1985).

[5] S. J. Gurman, N. Binsted, and I. Ross, J. Phys. C **17**, 143 (1984); S. J. Gurman, N. Binsted, and I. Ross, *ibid.* **19**, 1845 (1986).

[6] (a) J. E. Müller and W. L. Schaich, Phys. Rev. B **27**, 6489 (1983); (b) W. L. Schaich, *ibid.* **29**, 6513 (1984).

[7] J. J. Rehr, R. C. Albers, C. R. Natoli, and E. A. Stern, Phys. Rev. B **34**, 4350 (1986); see also, J. J. Rehr, Proc. SPIE **690**, 2 (1986).

[8] A. G. McKale, G. S. Knapp, and S.-K. Chan, Phys. Rev. B **33**, 841 (1986).

[9] J. J. Barton and D. A. Shirley, Phys. Rev. B **32**, 1906 (1985).

[10] D. E. Sayers, F. W. Lytle, and E. A. Stern, *Advances in X-ray Analysis* (Plenum, New York, 1970), Vol. 13, p. 248; J. J. Barton and D. A. Shirley, Phys. Rev. B **32**, 1892 (1985).

[11] A. Messiah, *Quantum Mechanics* (North-Holland, New York, 1966), especially Appendixes B and C.

[12] D. Arvanitis, K. Baberschke, and L. Wenzel, Phys. Rev. B **37**, 7143 (1988); J. J. Boland, S. E. Crane, and J. B. Baldeschwieler, J. Chem. Phys. **77**, 142 (1982).

[13] M. Danos and L. Maximon, J. Math. Phys. **6**, 766 (1965).

[14] R. Nozawa, J. Math. Phys. **7**, 1841 (1966).

[15] J. J. Barton and D. A. Shirley, Phys. Rev. A **32**, 1019 (1985).

[16] R. C. Albers and J. J. Rehr (unpublished).

[17] P. Lloyd and P. V. Smith, Adv. Phys. **21**, 69 (1972).

[18] A. R. Edmonds, *Angular Momentum in Quantum Mechanics* (Princeton University Press, Princeton, 1968).

[19] M. Sagurton, E. L. Bullock, R. Saiki, A. Kaduwela, C. R. Brundle, C. S. Fadley, and J. J. Rehr, Phys. Rev. B **33**, 2207 (1986).

[20] J. Mustre, J. J. Rehr, C. R. Natoli, C. S. Fadley, and J. Osterwalder, Phys. Rev. B **39**, 5632 (1989).